Two-layer Modeling of Smoke Movement in Building Fires

E. E. Zukoski and Toshi Kubota
Department of Jet Propulsion and Mechanical Engineering and Department of Aeronautics, California Institute of Technology, Pasadena, California 91125, USA

A description is given of a model which predicts the motion of combustion products and fresh air caused by a fire located in one room of a two-room structure. The gas in each room is assumed to be divided into two homogeneous layers, a layer next to the ceiling which contains hot combustion products and one next to the floor which contains fresh air. The model predicts the motion of the interface separating these layers and the density of the hot layers as a function of time and an arbitrarily specified fire heat release rate.

INTRODUCTION

A fire starts in a room of a multiroom structure. Hot gas rises from the fire, entrains fresh air from the room as it rises toward the ceiling in a buoyant plume, and forms a distinct layer of hot gas under the ceiling. This ceiling layer of hot gas gradually becomes thicker and finally starts to flow out under the door soffit into the next room. Under the influence of heat transfer from the fire and ceiling layer gas, the fire heat input grows and combustible material surrounding the fire is gradually heated. Finally, some minutes after ignition, these uninvolved fuel elements begin to pyrolyze rapidly, fire spreads through the combustible products of pyrolysis and room flashover occurs.

During the early stages of this process the heat released by the fire keeps the pressure in the room above that in adjoining rooms, and both hot combustion products and unheated air flow out of the door. Later on, the pressure may fall below the ambient value. Then, fresh air can enter the room through the lower part of the door, to replace that entrained in the plume, and the hot combustion products will be able to flow out of the upper part of the door.

The hot gas flowing out of the fire room forms a ceiling layer of hot products in the adjoining room which becomes deeper until hot gas can flow on into other rooms further from the fire.

The spread of combustion products and fire described above is a complicated phenomenon which involves many interacting physical processes. These include the flow of products of combustion and fresh air into and out of the rooms affected by the fire, the transfer of heat by radiation and convection, the growth of the area involved in flaming combustion, pyrolysis of unignited fuel elements, ignition of the products of pyrolysis, etc. We have been interested in the fluid dynamic aspects of the overall fire spread problem and in the present paper we describe a model which predicts the motion of the combustion products and fresh air which is caused by a fire in one room of a two-room structure. The rooms are joined through a single rectangular opening of arbitrary elevation, height and width, and each room may have rectangular openings to the outside of arbitrary number, height, width and elevation.

We have restricted our solution to the period prior to flashover. During this period the hot products of combustion are usually so sharply stratified that we believe it is useful to divide the room into two distinct layers: a hot layer next to the ceiling called here the ceiling layer, and a cooler layer next to the floor. In our analysis we ascribe a single temperature and density to each layer, and the purpose of the calculations described here is to follow the changes in layer thickness and density during the course of a fire. This two-layer model is a rough approximation of the actual temperature profiles observed in real fire situations and its use greatly simplifies the calculations without losing the essential features of the process.

We do not attempt to calculate many important features of the fire. For example, we shall treat as *given* functions of the time, the fire heat input rate and the heat transfer rates from various regions of the gas. We have ignored the spreading process of the thin hot gas layer along the ceiling immediately following the impingement of the fire plume or the door plume in the adjacent room. Instead, in keeping with the two-layer model, we assume that the hot gas spreads instantaneously over the ceiling as soon as the plume hits it.

The model described here is part of a continuing program for the development of a fire spread model which is being carried out under the auspices of the Fire Research Center of the National Bureau of Standards.

The two-layer model has its origin in the work of Kawagoe (e.g. Ref. 1) who studied the flow of gas through an opening connecting a region containing gas with uniform temperature and composition (i.e. a single layer) to a fire room which was treated as a well-stirred reactor which contained gas at a different uniform temperature and composition. Later, P. H.

CCC–0308–0501/80/0004–0017 $05.50

Thomas and co-workers (e.g. Ref. 2) studied flows in which there was a well-defined stratification of hot and cold gas within a single compartment.

The ideas behind the present two-layer room models have been discussed previously at many meetings and in a number of papers (e.g. Refs. 3 and 4). Other papers dealing with the application of the model are given in Refs. 5–8. The computer model described here puts these ideas into a simple numerical program, extends current programs to a two-room configuration and extends several of the models of physical processes.

We shall describe the physical basis for our model and typical results, but shall not go into details of the computation here. A complete description of the computer program is given in Ref. 9.

PHYSICAL BASES FOR MODELING

Several elements of the present model are described in this section. These are: the fire plume, a turbulent buoyant plume in which cool air is entrained, heated and transported to the ceiling layer; the flow through openings under the influence of a hydrostatic pressure field; and entrainment by the gas flowing through the opening. Given mathematical models for these elements and the equations for conservation of mass and energy for each layer, we have developed a numerical calculation for the pressure, temperature, density and height of each layer in the two-room model. Generalization of the model to include more rooms is presently in progress.

In the following paragraphs we give a brief derivation of the conservation laws and describe the physical bases for the mathematical models of other flow phenomena.

Equations of conservation of mass and energy

Suppose that a fire with heat release rate Q is burning in room 1, and that room 2 is connected to room 1 through one opening. Rooms 1 and 2 may have other openings to the outdoors. The geometry and symbols are shown in Fig. 1 and symbols are defined in the Appendix. Equations for mass and energy balance for the ceiling layer and the lower layer in room 1 are given below. Equations (1) and (2) are the continuity equations, and (3) and (4) are equations for the internal energy of the gas in each layer. The dy_1/dt terms in (3) and (4) are included to account for the work done by pressure forces on the moving interface between the two layers.

$$\frac{d}{dt}(\rho_1 y_1 S_1) = \dot{m}_1 - \dot{m}_E \tag{1}$$

$$\frac{d}{dt}[\rho_{h1}(h_1 - y_1)S_1] = \dot{m}_E + \dot{m}_f + \dot{m}_{h1} \tag{2}$$

$$\frac{d}{dt}(\rho_1 y_1 S_1 C_v T_1) + p_1 S_1 \frac{dy_1}{dt} = \dot{q}_1 - \dot{m}_E C_p T_1 \tag{3}$$

$$\frac{d}{dt}[\rho_{h1}(h_1 - y_1)S_1 C_v T_{h1}] - p_1 S_1 \frac{dy_1}{dt} = \dot{m}_E C_p T_1 + Q - \dot{q}_{h1} \tag{4}$$

In these equations, $\dot{m}_1$ and $\dot{m}_{h1}$ are the algebraic sums of all mass flows through openings into the layer in question. Also, $\dot{q}_1$ and $\dot{q}_{h1}$ represent the sums of (a) enthalpy fluxes through the openings and (b) heat transfer by convection and radiation *into* the respective regions. The mass flow entrained by the plume in the lower layer and transported into the upper layer is $\dot{m}_E$ and fuel flow rate is $\dot{m}_f$.

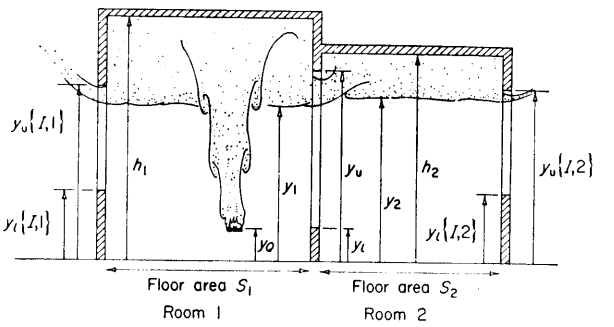

Figure 1. Schematic diagram for two-room model to illustrate notation.

The static pressure within a room varies because of hydrostatic effects by terms of the order of ρgh and thus errors of the order of ρgh compared to a mean value p_1 are made if the hydrostatic terms are omitted. However, the ratio of hydrostatic pressure to static gas pressure is very small. Thus, for a room height h of 2.5 m,

$$\frac{\rho gh}{p_1} < \frac{\rho_\infty gh}{p_1} < 3 \times 10^{-4}$$

Hence we can neglect these hydrostatic effects in the equations of state, which may be written as

$$\rho_1 R T_1 = p_1 \quad \text{and} \quad \rho_{h1} R T_{h1} = p_1 \tag{5}$$

We have also assumed here that the gas constants R_h and R are equal. When we replace $(\rho_1 T_1)$ and $(\rho_{h1} T_{h1})$ by p_1/R in Eqns (3) and (4), and add the resulting equations, we obtain an equation for p_1 of the form

$$\frac{dp_1}{dt} = \frac{R}{C_v S_1 h_1}(\dot{q}_1 + \dot{q}_{h1} + Q) \tag{6}$$

The temperature and hence the density in the lower region changes with pressure changes in the room and also because of heat transfer to the gas in the lower layer. The relative magnitude of the pressure variation is small in many cases of practical interest. The heat transfer to the lower layer air is produced by mixing between hot and cold gas flows at openings, and by convective heat transfer from the floor and walls that are heated by radiation from the fire, from the hot ceiling layer gas, and from the walls and ceiling in contact with the ceiling layer gas. In the first few minutes of a fire these effects are often small, and when these effects are negligible, T_1 and ρ_1 are equal to the temperature and density of the ambient air, i.e. to T_∞ and ρ_∞ respectively. For simplicity, this assumption is made in the numerical program described here. (The more complete problem is also being programmed.)

Given these simplifications, the system of differential equations (1), (2) and (6) reduces to

$$\rho_\infty S_1 \frac{dy_1}{dt} = \dot{m}_1 - \dot{m}_E \tag{7}$$

$$S_1 \frac{d}{dt}[(h_1 - y_1)\rho_{h1}] = \dot{m}_E + \dot{m}_f + \dot{m}_{h1} \tag{8}$$

$$\frac{dp_1}{dt} = \frac{R}{C_v S_1 h_1}(\dot{q}_1 + \dot{q}_{h1} + Q) \tag{9}$$

A similar set of equations can be developed for the two layers in room 2. Thus, six conservation equations plus two equations of state are available to solve for the eight unknowns: ρ_{h1}, T_{h1}, y_1, p_1, and ρ_{h2}, T_{h2}, y_2, p_2.

However, before solving these equations we must be able to specify the dependence on these eight variables of the heat and mass flux terms, such as $\dot{q}_{h1}$ and $\dot{m}_{h1}$. These flow processes are described in the following paragraphs.

Entrainment by fire plume

The primary source of entrainment is the fire plume which acts as a pump to move air up into the ceiling layer. The fire plume is well enough understood for the entrainment rate produced by physically small fires (for which the heat release region lies beneath the ceiling layer) to be described adequately. Larger fires (which penetrate the ceiling layer) cannot yet be treated with any confidence. At present we use the conventional Boussinesq treatment, described here, for all fires regardless of size. This model is adequate for small fires.

This fire plume model is based on that described by Morton *et al.*[10] and it makes use of the Boussinesq approximation that density differences are small enough to be ignored everywhere except in the buoyancy terms of the momentum equation. One free parameter is available to fix the rate of entrainment of fresh air by the plume. When the experimental results of Yokoi[11] are used to determine the constant that appears in the entrainment assumptions, the turbulent fire plume can be characterized by the following equations:

$$\frac{\Delta T_m}{T_\infty}=\frac{\Delta\rho_m}{\rho_\infty}=C_T(Q^*)^{2/3} \qquad C_T\approx 9.1$$

$$\frac{w_m}{\sqrt{gZ}}=C_v(Qz^*)^{1/3} \qquad C_v\approx 3.8$$

$$\frac{l_v}{Z}=C_l \qquad C_l=0.125$$

$$\frac{l_t}{Z}=C_l \qquad \frac{C_{l_t}}{C_l}=1.15$$

and

$$\frac{\Delta T}{\Delta T_m}=\exp\{-(r/l_t)^2\}$$

$$\frac{w}{w_m}=\exp\{-(r/l_v)^2\}$$

Here the subscript m refers to conditions on the centerline of a plume with Gaussian distribution of velocity w, temperature T and density ρ. Length scales for the radial distribution of temperature differences $\Delta T\equiv T-T_\infty$ and velocity are l_t and l_v. The parameter Qz^* is a dimensionless measure of the rate of heat input from the fire, $\dot{Q}$, and height above the fire Z. It is defined as

$$Qz^*=Q/(\rho_\infty\sqrt{gZ}\,C_pT_\infty Z^2) \qquad (10)$$

Measurements made above the visible flame of a fire, and where Z is large compared with the diameter of the fire D, are in good agreement with the predictions made from this representation (see Refs. 11 and 12).

Given these approximations, we can show that the mass-averaged temperature and density in the plume are

$$\frac{\overline{\Delta T}}{T_\infty}=\frac{\overline{\Delta\rho}}{\rho_\infty}=\left(\frac{1}{\pi C_v C_l^2}\right)(Qz^*)^{2/3}=\frac{Q}{\dot{m}_E C_p T_\infty}$$

and mass flow in the plume at height Z is

$$\dot{m}_E=\rho_\infty w_{max}\pi l_v^2$$

or

$$\dot{m}_E=\rho_\infty\sqrt{gZ}\,(Qz^*)^{1/3}Z^2(\pi C_v C_l^2) \qquad (11)$$

A development similar to that outlined above for the axisymmetric plume can be carried out for the plume above a line fire. The only new parameter is the fire length L and we again use a dimensionless heat addition parameter Q_2^* which is based on the total heat released by the fire and elevation:

$$Q_2^*=\frac{Q}{\rho C_p T_\infty\sqrt{gZ}\,LZ}$$

where Q = total heat addition rate. The plume equations are based on the assumption of a Gaussian distribution for velocity and temperature with a scale l_v. The model equations are

$$\frac{\Delta T_{m2}}{T_\infty}=C_{T2}(Q_2^*)^{2/3} \qquad C_{T2}=2.6$$

$$\frac{w_{m2}}{\sqrt{gZ}}=C_{v2}(Q_2^*)^{1/3} \qquad C_{v2}=2$$

$$\frac{l_v}{Z}=C_{l2} \qquad C_{l2}=0.14$$

$$m_{E2}=\rho_\infty\sqrt{gZ}\,ZLQ_2^{*1/3}(\sqrt{\pi}\,C_{v2}C_{l2})$$

$$\frac{\overline{\Delta T}}{T_\infty}=(\sqrt{\pi}\,C_{v2}C_{l2})(Q_2^*)^{2/3}=\frac{\overline{\Delta\rho}}{\rho_\infty}$$

The values of constants are much less certain here than for the axisymmetric case, and again, the Boussinesq approximation has been used.

Entrainment at an opening

Entrainment at an opening is even less well understood. We describe here several entrainment processes and discuss the *ad hoc* entrainment model used in the present computer program; clearly, a more complete description must be developed. Two situations in which strong entrainment at an opening have been observed are illustrated in Fig. 2. In Fig. 2(a) we show a situation in which pressure differences across an opening cause a jet of hot gas to flow under the soffit of an opening and impinge on the ceiling layer of an adjacent room. The jet entrains gas from the cooler region of the second room during this process and under some conditions the entrained flow will be larger than the flow through the door.

A number of regimes of flow must be taken into account if we are to model this phenomenon accurately. Two additional situations are shown in Fig. 3. When hot fluid begins to flow through the door, the door jet usually stays attached to the wall (see Fig. 3(a)) and entrains fluid on one side only. As the depth of the flow at the door (y_u-y_1) increases, the flow separates from the wall (see Fig. 2(a)) and entrains fluid on both sides. A third type of flow which occurs when the depth of the hot layer in room 2 is very shallow is illustrated

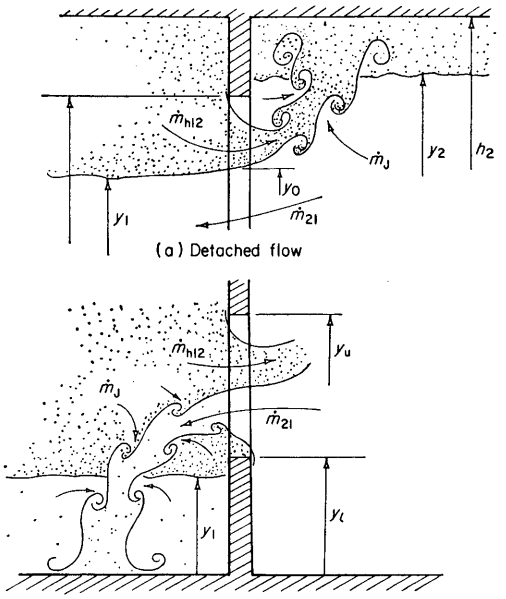

Figure 2. Mixing in the opening.

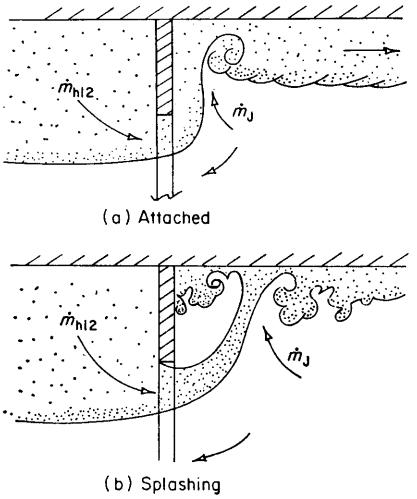

Figure 3. Door mixing regimes.

in Fig. 3(b). The door-jet flow (attached or detached) splashes energetically through the thin ceiling layer and produces a very rapid mixing of door jet and cool layer material in a process similar to a hydraulic jump.

We are still developing models to describe these mixing processes and to specify the conditions under which transition between these regimes will occur. In the present calculation we include only a model for the detached jet without splashing.

Parallel situations exist when a flow from a lower or cool layer enters an adjoining room. One case is shown in Fig. 2(b). We use the same type of model for these flows as for the previous examples.

Based on salt-water modeling work, we conclude that the characteristic dimension for the flow shown in Fig. 2(a) is the depth $Z_d \equiv (y_2 - y_0)$, where y_0 is the elevation in the doorway where the pressure difference across the door is zero. For shallow plumes in large doors, $y_0 \approx y_1$. The water model tests suggest that the entrainment can be estimated by assuming that the door jet acts like a simple, point source buoyant plume. Thus, the experimental data obtained in salt-water/water tests indicates that

$$\dot{m}_J = (C_J)\rho_2 \sqrt{gZ_d}\, Z_d^2 (Q_d^*)^{1/3}$$

where we use as an analog for Q^* the term

$$Q_d^* = (\dot{m}_{h1} C_p (T_{h1} - T_2))/\rho_2 C_p T_2 \sqrt{gZ_d}\, Z_d^2$$

Model experiments suggest that $C_J = 0.30$ for the separated case and $C_J = 0.18$ for the attached flow. Compare this description with Eqn (10) used for the axisymmetric buoyant plume.

The experimental work used to develop this correlation is described in Ref. 13 and is preliminary in nature. Nevertheless, the correlation was satisfactory for geometries in which we expected that the line source would make a more reasonable approximation. This rather unlikely result certainly needs further experimental confirmation, but it will be used here until a better description is available.

When these equations are combined, we find that

$$\frac{\dot{m}_J}{\dot{m}_{h1}} = C_J \left(\frac{\rho_{h1} - \rho_2}{\rho_2}\right)(Q_d^*)^{-2/3} \qquad (12)$$

In the present program $C_J = 0.3$ is used because the transition process between the various regimes is not yet understood.

Flow through an opening

Calculation of flows through an opening connecting spaces with differing static pressures is approached in the same manner as that used to calculate flow through an orifice. Based on an analogy with orifice flow, the mass flux from room i to room k through an opening of area A and due to pressure difference $(P_i - P_k)$ is assumed to be

$$\dot{m}_{ik} = \rho_i V_i C_{0i} A = C_{0i} A \sqrt{2(P_i - P_k)\rho_i}$$

The coefficient C_{0i} is the flow coefficient which accounts for the ratio of the cross-section area at the vena contracta of the jet to the area of the opening and also accounts for errors in this simple calculation due to viscous effects and other geometric effects. The computer program is written to make i lie on the side of the opening which has the higher pressure. Hence $(P_i - P_k)$ will always be positive and no trouble is encountered in evaluating the square root in this equation.

In many flows through openings the pressure difference is a function of elevation due to differences in the densities of the gas on either side of the opening. In these cases we assume that the above equation can be used in a differential form and can then be integrated to obtain the total mass flow. Thus, we assume that

$$\frac{d\dot{m}_{ik}}{dA} = C_{0i}\sqrt{2(P_i - P_k)\rho_i}, \text{ that } dA = b(y)\, dy,$$

and the corresponding mass flow rate is

$$\dot{m}_{ik} = C_{0i} \int_{y_l}^{y_u} \sqrt{2(P_i - P_k)\rho_i}\, b(y)\, dy \qquad (13)$$

Here, $b(y)$ is the width of the opening, y is the vertical coordinate and g the gravitational constant. The integral is taken over the region between the highest (or upper) extent of the door y_u and the lowest extent y_l. The pres-

sure difference can be written as a function of elevation y, the densities and the values of pressure at $y=0$ as

$$(P_i-P_k)=(P_{i0}-P_{k0})-\int_0^y(\rho_i-\rho_k)g\,dy=\Delta P_{ik} \quad (14)$$

To summarize this process, we assume that flow through an opening is dominated by the hydrostatic pressure field within either room and that at any elevation the mass flux through an opening can be calculated as if the opening were a small orifice which does not affect the pressure field.

The pressure difference across the wall separating two rooms can change in sign as we move from the floor to the ceiling for physically reasonable flow situations. For instance, consider the example shown in Fig. 4. Here, each room is assumed to be divided into two regions; the density of the gas in the two lower regions is ρ_∞, and in the upper regions is ρ_{h1} and ρ_{h2} respectively. In addition, we have assumed that $\rho_\infty>\rho_{h2}>\rho_{h1}$. The pressure difference across the wall which is produced by hydrostatic effects when the pressure difference at the floor is negative is shown in Fig. 4. Between the floor and elevation y_1 the density difference is zero and we see from Eqn (14) that the pressure difference must be constant. Between y_1 and y_2 the density difference $(\rho_{h1}-\rho_\infty)$ is negative and consequently the pressure difference must increase. The position of zero difference is at y_0 and it is called the neutral buoyancy point. Above y_2 the density difference $(\rho_{h1}-\rho_{h2})$ is still negative but we have assumed it to be less so and hence the slope is larger in this region.

The direction of mass flow through an opening in the situation described in Fig. 4(a) will be from room 2 to room 1 if the opening is below y_0 and in the opposite direction if it is above y_0. Both flows can be calculated from Eqn (8) and the choice of subscripts i and k, and the direction of the flow, will be fixed according to the sign of the pressure difference.

Rather than carrying out numerical integration of terms such as those in Eqns (13) and (14) for each opening and each time step, we have chosen to carry out the integrals analytically for all possible cases. For example, consider the situation shown in Fig. 4(b) where an opening has its upper bound in region II and lower in region IV, and has a constant width b. The mass flux for the region $y_l\leqslant y<y_0$ is from room 2 into room 1 and is

$$\dot m_{21}=C_{02}\sqrt{-2\Delta P_0\rho_\infty g}\,b(y_1-y_l)+\frac{2\sqrt2}{3}C_{02}b\sqrt{\rho_\infty g(\rho_\infty-\rho_{h1})}\,(y_0-y_1)^{3/2} \quad (15)$$

where the first term of this equation is given by the integral over region IV and the second by that over region III. The value for y_0 is

$$y_0=y_1-\Delta P_0/[(\rho_\infty-\rho_{h1})g]$$

where ΔP_0 is $(P_{10}-P_{20})$ and has a negative value for our example and hence $y_0>y_1$.

Similar algebraic relationships have been developed for the flow out of the hot region of room 1 into the hot region of room 2. For the special case considered in Fig. 4(b) the flow through the opening between y_0 and y_u is

$$\dot m_{h12}=\frac{2\sqrt2}{3}C_{01}b\sqrt{\rho_{h1}(\rho_\infty-\rho_{h1})}\,(y_u-y_0)^{3/2} \quad (16)$$

Because y_0 is a function of ΔP_0, it is clear that all three terms in Eqns (15) and (16) depend on ΔP_0 as well as the densities in the hot layers and the interface elevations.

In order to specify mass flow rate expressions for use in the computer program, we must write algebraic equations such as (15) and (16) for each of the possible locations of the upper and lower boundaries of the opening with respect to y_1, y_0 and y_2. In each of ten examples, algebraic expressions such as those given in Eqns (15) and (16) have been developed for the mass flux and are stored in the computer program. The table shown in Fig. 4 specifically identifies the ten configurations we must be able to handle. For instance, when y_u is in region II (between y_2 and y_0) and y_l is in region III (between y_0 and y_1) the configuration is identified as 1.1.2.2. The example shown in Fig. 4(b) is case 1.1.2.1.

For cases in which the opening geometry includes the neutral buoyancy point, flow in both directions will be present. This situation is illustrated in Fig. 4(b) for the example discussed above. The geometry of the flow near the door is complex and we expect that some dependence of the flow coefficient on opening geometry will occur to produce deviations from our simple model.

Extensive model measurements (e.g. Ref. 14) have demonstrated that the flow field sketched in Fig. 4(b) is a reasonable model for real flows, and suggest that values of the flow coefficients for such flows lie between 0.6 and 0.7 as long as the Reynolds number of the flow is above a few thousand. We use 0.6 in the present calculations. We believe that the low values reported in Ref. 14 are a result of surface tension effects which were overlooked in that work.

We have assumed in drawing the pressure vs. elevation curve shown in Fig. 4 that the density in the ceiling layer of room 2 is greater than that in room 1, i.e. that $\rho_{h1}\leqslant\rho_{h2}$. Two other variations of the pressure distribution are possible with this density distribution and these are shown in Fig. 5. In case 2 (Fig. 5(a)) the neutral buoyancy point y_0 lies above y_2, whereas in case 1 (Fig.

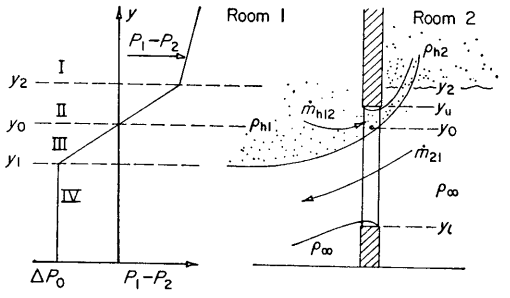

(a) Pressure distribution in various zones

(b) Flow field when y_u is in zone II

y_l \ y_u	I	II	III	IV
I	1.1.1.4			
II	1.1.1.3	1.1.2.3		
III	1.1.1.2	1.1.2.2	1.1.3.2	
IV	1.1.1.1	1.1.2.1	1.1.3.1	1.1.4.1

Figure 4. Opening flow calculation scheme.

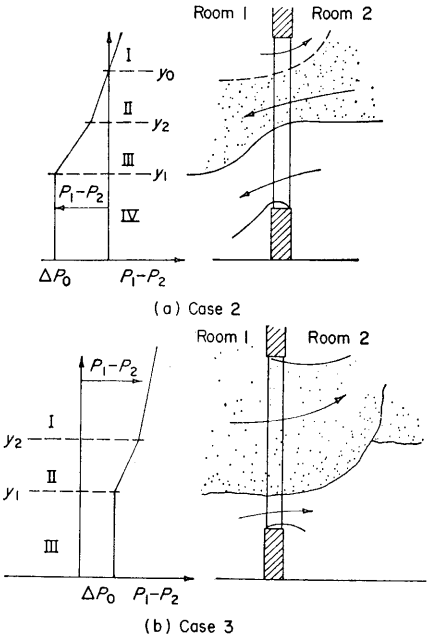

Figure 5. Opening flow calculation scheme, cases 2 and 3.

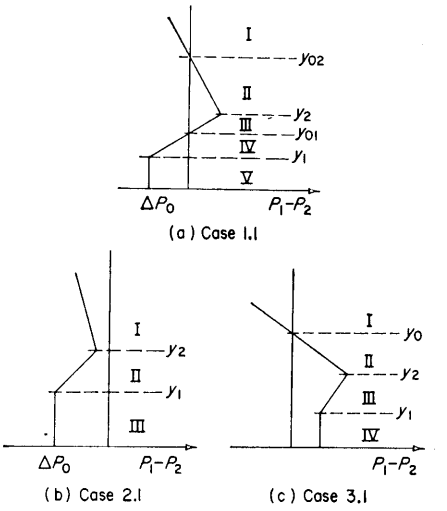

Figure 6. Opening flow calculation scheme for $\rho_{h1} > \rho_{h2}$.

4) it lies between y_1 and y_2. For the flow shown in Fig. 5(b) the pressure in room 1 is greater than that in room 2 at the floor level.

Bookkeeping of a new type must be developed to account for the complex flow of case 2. Here, hot gas flows out of the hot region of room 1 into the hot region of room 2 for $y > y_0$. We also have a hot flow from room 2 back into room 1 for $y_0 > y > y_2$. Finally, a cool flow moves from the lower region of room 2 to the cool region of room 1 for $y_2 > y > y_1$. The hot gas flowing into room 1 from room 2 in situations like this may form a third region of intermediate density in room 1 when ρ_{h2} and ρ_{h1} are appreciably different. In our treatment of this flow, however, we arbitrarily assume that the flux of hot gas from room 2 into room 1 (for $y_0 > y > y_2$) flows into and mixes instantaneously with the hot gas in the upper layer of room 1. Experimental work is required to check the validity of these flow field assumptions.

The flow field and calculations of the situation described in Fig. 5(b) are relatively straightforward and approach closely to conventional orifice flows.

We must also deal with situations in which the density inequality is reversed, i.e. when $\rho_{h1} > \rho_{h2}$. This change in density distribution will primarily affect the sign of the slope of the pressure vs. elevation curves for positions above y_2. Pressure distributions for the three cases we need to examine are shown in Figs. 6(a), 6(b) and 6(c). Note that case 1.1 corresponds to case 1, case 2.1 to case 2, and case 3.1 to case 3 with the exception that the slope of the line for $y > y_2$ changes sign.

Finally, we must consider situations in which the ceiling layer in room 2 is below that in room 1. For this situation, the computer has been instructed to reverse the indices 1 and 2, and calculate mass fluxes as before.

The mass flow rates corresponding to the conditions described by the pressure distribution shown in Figs. 5 and 6 have been treated in the same manner as the example shown in Fig. 4. Equations similar to Eqns (14) and (15) have been developed and their integrals are included in the computer program. In all, 64 cases must be considered.

Given the mass flux results, we can calculate values for the parts of $\dot{q}_1$ and $\dot{q}_{1h}$ which correspond to the enthalpy fluxes. For instance, let us return to the example shown in Fig. 4. For this case

$$(\dot{q}_1)_{door} = (\dot{m}_{21}) C_p T_\infty$$

$$(\dot{q}_{h1})_{door} = -(\dot{m}_{12}) C_p T_{h1}$$

where $\dot{m}_{21}$ is the sum of the expressions given in Eqn (15) and $\dot{m}_{h12}$ is the expression given by Eqn (16). Similar flux terms can be evaluated for each opening using these equations to derive the appropriate mass flux terms.

The $\dot{q}_i$ terms also include conduction and radiant heat fluxes. In the present program these must be given as specified functions of the time. However, when better models are available they can easily be included in the program.

Quasi-steady-state approximation

We return now to the conservation relation given in Eqn (6), and make one further approximation—that the dP/dt term is negligible. This approximation can be justified by comparing the magnitudes of the terms in Eqn (6) when the mass and energy flux terms are specified by use of equations such as (19) or (20).

We can also proceed by noting that when room pressures rise to one hundredth of one atmosphere above the pressure in the ambient atmosphere, velocities of the order of many tens of meters per second will be produced through openings connecting the rooms with the atmosphere. Since velocities of this order are only observed under unusual circumstances, we conclude that pressure differences will be kept to values so small that pressure variations around the ambient value will have a negligible effect on gas density and temperature. This question is discussed in more detail in Ref. 8.

The conservation equations for each room are reduced to a set of two nonlinear first-order equations given in

Eqns (7) and (8) and one algebraic equation:

$$\dot{q}_i + \dot{q}_{hi} + Q = 0 \qquad (17)$$

The plume and door-jet entrainment rates are specified in previous sections. The parts of the $\dot{q}_i$ terms which are enthalpy fluxes can be calculated from the opening mass flow calculations and the appropriate C_pT terms; the heat transfer terms must be given as specified functions of the time. Finally, the equation of state can be used to relate pressure, density and temperature. Although considerable bookkeeping is required here, the procedure is straightforward.

The six independent variables are the pressures, ceiling layer densities and interface heights in the two rooms.

COMPUTER PROGRAM

Numerical solution of the four ordinary differential equations and the two nonlinear algebraic equations for pressures, ceiling layer heights and densities are coded in FORTRAN IV to be executed by an IBM 370 computer at the CIT Computing Center.

At each time step the nonlinear algebraic equations are solved by a numerical Newton's method to obtain the pressures and hence the mass and energy fluxes through the openings, and then the differential equations are solved by a CIT library routine which incorporates the fourth-order Runge–Kutta–Gill method, the Adams–Moulton predictor–corrector formula and a provision for automatic control of truncation error. Details of the computer program are described in Ref. 9.

DISCUSSION OF RESULTS

In this section we shall discuss the behavior of the ceiling layers in a number of one- and two-room configurations which are predicted by the program. Some results of general interest are obtained concerning the influence of several parameters and a number of examples are presented.

In presenting these results a modified time scale has been used which takes into account roughly the effect of fire heat input rate when the dimensionless heat input rate, based on room height Q^*, is less than 0.10. This dimensionless parameter is

$$t^* = (h\sqrt{gh}/S)t(Q^*)^{1/3}, \qquad Q^* \equiv \frac{Q}{\rho_\infty C_p T_\infty \sqrt{gh}\, h^2}$$

The aim of the examples presented here is to illustrate the output of the program, to show some features of the early stages of a fire which we believe occur in real fires and, in particular, to determine the duration or time scale of this early stage.

Consider first a two-room example which exhibits some of the capabilities of the program. The first room has a height h and is connected to the outside by a window which is almost closed but contains leaks which are modeled by an opening with $y_l = 0.4h$ and $y_u = 0.8h$ and a width $b = 0.0025h$. The door which connects the two rooms is almost closed at first; its width increases

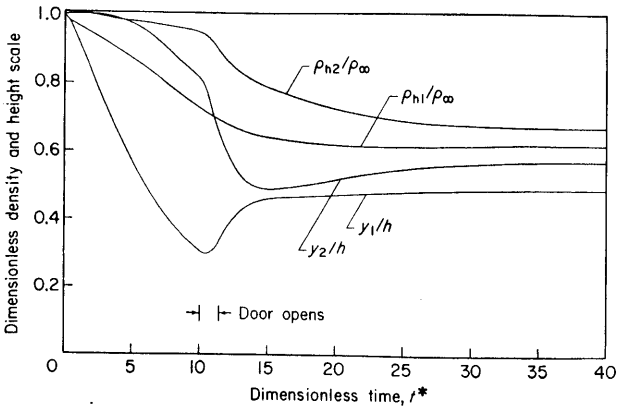

Figure 7. Two-room example.

linearly starting at $t^* = 10$ and it is completely opened at $t^* = 11.5$. The door top is located at $0.813h$ and for $0 \leqslant t^* \leqslant 10$ its width is $0.002h$. After $t^* = 11.5$, the door width is $0.375h$. Room 2 has the same area and height as room 1 and is connected to the outside by an open door with height $0.813h$ and width $0.375h$.

The fire grows linearly from a very small value at $t^* = 0$ to a value corresponding to $Q^* = 0.01$ at $t^* = 8$ and remains constant thereafter. Heat losses to the walls from the hot layer in room 1 are 25% of the fire heat input rate, and in room 2 they are 20% of $(\dot{m}_{h12})C_p(T_{h1} - T_\infty)$, i.e. the net enthalpy flux of the hot flow through the door from room 1.

The dimensionless ceiling layer interface heights y_i/h and density ratios for the ceiling layers ρ_{hi}/ρ_∞ are shown in Fig. 7. The ceiling layer interface height and density in room 1 fall rapidly for $t^* > 0$ and continue to decrease until the door opens. Small changes occur in the second room after $t^* = 2.4$ when the ceiling layer in room 1 falls below the soffit of the door connecting rooms 1 and 2. As the door is opened, a rapid flow of hot gas enters room 2 and the steady-state values of the parameters are very nearly reached at $t^* = 20$.

In order to put these parameters in dimensional form we must assign values to room height, etc. When we pick: height $= h = 2.5$ m, floor area $\equiv S = 20$ m^2 and $T_\infty = 20$ °C, then

$$\text{heat input} = Q = Q^*(1.11 \times 10^4 \text{ kW}),$$

and the steady value is 111 kW;

$$\text{time} = t = (t^*) \times (7.5 \text{ s}).$$

For these values, note that when the door is opened at about 75 s after the start of the fire, the temperature in the ceiling layer of the first room is already about 90 °C and that the interface of this layer is at about 0.8 m above the floor level. The time required after the door is opened for the excess hot gas in room 1 to flow into room 2 is about 40 s. Final ceiling layer temperatures are about 200 °C.

In the following paragraphs we shall first examine the effects of changing some of the parameters which appear in our program and then give a number of examples.

Entrainment parameters and flow coefficients

A number of constants appear in the fire plume and door flow modeling equations and it is of interest

Table 1. Effect of changing flow coefficients for flow through opening[a]

Q^*							
	$C_{0h}=$	0.6	0.7	0.8	1.0	0.6	1.0
	$C_{0c}=$	0.6	0.7	0.8	1.0	1.0	0.6
10^{-5}	y_1/h	0.585	0.600	0.612	0.613	0.590	0.625
	$\left(100\,\frac{(\rho_\infty-\rho_{h1})}{\rho_\infty}\right)$	0.604	0.578	0.558	0.520	0.595	0.530
10^{-2}	y_1/h	0.560	0.577	0.591	0.613	0.566	0.604
	$\left(\frac{(\rho_\infty-\rho_{h1})}{\rho_\infty}\right)$	0.396	0.384	0.374	0.360	0.391	0.366

[a] Values for $y_u/h=0.813$ and $b/h=0.375$.

to compare the sensitivity of the ceiling layer depth and density to changes in these parameters. In particular, we are concerned with the sensitivity of the solutions to the choice of flow coefficients for the flow through the openings and the entrainment parameters for the plume and the door jet. We shall examine the influence of the first two parameters for a single room which has a single door opening to the outside, and which has a soffit at $0.813h$ and a width of $b=0.375h$.

Experimental data suggest that the values for the two orifice coefficients, C_{0c} and C_{0h}, which appear in equations for the door flows, should lie in the range 0.6–1.0 and that for many configurations of interest the value is close to 0.60. The effects of changes in these coefficients on the hot layer density and ceiling layer thickness are illustrated in Table 1. Here, steady values of interface height and ceiling layer density are presented as a function of Q^* and the flow coefficients. The steady values were obtained for dimensionless times of the order of 40 in all cases. Flow coefficients in the range 0.6–1.0 and for Q^* values of 10^{-5} and 10^{-2} are considered.

Changing both coefficients simultaneously from 0.6 to 1.0 causes the ceiling layer interface height y_1 to increase by less than 10%. The density ratio (ρ_{h1}/ρ_∞) for the smaller value of Q^* is very close to 1 and the quantity $(\rho_\infty-\rho_{h1})/(\rho_\infty)$ is used for both cases to make the changes easier to perceive. This density difference ratio decreases by less than 14% as the coefficients increase from 0.6 to 1.0 for both values of Q^*, and this change is a result of the increase in y_1 which increases the entrainment in the plume and hence decreases the plume mass-averaged temperature. The last two columns of the table illustrate the changes produced when the coefficients are not of equal value.

The variations in the interface level y_1 and density of the ceiling layer produced by a wide range of values of flow coefficients are less than ±6% for the conditions considered here. Hence, our solutions will not be critically dependent on the accuracy of the value used in our computations. We shall use 0.60 for both coefficients.

The effects of changing the plume entrainment rate constant, $C_E\equiv(\pi C_v C_l^2)$ (which appears in Eqn (11)), on the interface height and ceiling layer density are shown in Table 2 for the same room and fire uses in the above example and with $Q^*=0.01$. Clearly, changing C_E by factors of 2 produces appreciable changes in both parameters and hence C_E must be known to within ±50% to avoid serious errors. The value used in the other calculations described here is $C_E=0.1865$ which is satisfactory for describing the far field of ideal fires, i.e. the plume above an undisturbed fire.

Table 2. Effect of changing entrainment rate parameter C_E[a]

$C_E=$	0.046	0.093	0.1865	0.373	0.746
y_1/h	0.71	0.65	0.56	0.45	0.33
$\frac{\rho_\infty-\rho_{h1}}{\rho_\infty}$	0.64	0.51	0.40	0.32	0.29
$\frac{C_E}{C_{ES}}$	$\frac{1}{4}$	$\frac{1}{2}$	1	2	4

[a] Values for $y_u/h=0.813$, $b/h=0.375$ and $Q^*=0.01$ as in Table 1.

Heat input rate, one room

The influence of the dimensionless heat input parameter Q^* on the transient behavior of the ceiling layer interface level and the density is shown in Fig. 8 for a single room with a single door. In this example the fire heat input rate is zero up to $t^*=0$, and is constant thereafter. For purposes of comparison, the density is presented as the ratio $DR\equiv(\rho_{h10}-\rho_{h1})/(\rho_{h10}-\rho_{h1s})$, where ρ_{h10} is the value when the plume first reaches the ceiling, ρ_{h1} is the instantaneous value of ceiling layer density, and ρ_{h1s} is the ceiling layer density after the steady state has been achieved. The time scale is the parameter t^*.

In this figure, curves for values of Q^* of 10^{-4}, 10^{-3}, 10^{-2} and 10^{-1} are shown. For the lowest three values of Q^* the time scale used here, t^*, does a reasonable

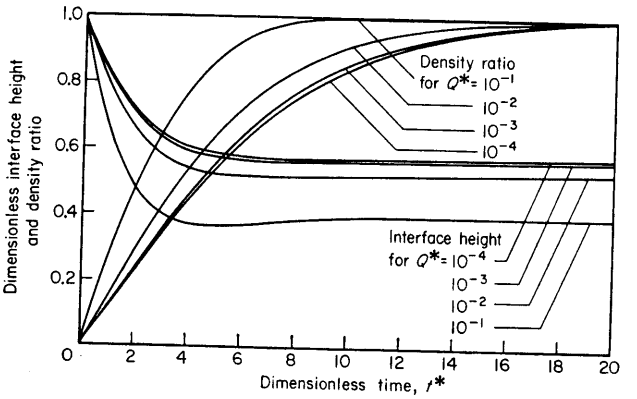

Figure 8. Effect of Q^* on density ratio and interface height for a single room.

job of reducing the three curves to a single curve. Curves not shown here, for even smaller values of Q^*, are indistinguishable from the $Q^*=10^{-4}$ curves. Thus, t^* is a useful scaling parameter for small fires, and the appropriate time scale for this phase of the fire appears to be 5–10 for this room and door geometry. However, for $Q^* \geq 10^{-1}$ the simple scaling of the time is no longer satisfactory and large deviations occur.

Opening geometry

The effects of room scale, both floor area S and room height h, are contained within the dimensionless ceiling layer height $y_1=y_1/h$ and time scale t^*. Hence, the results presented in Fig. 8 are general with respect to these parameters. However, the door geometry which is described by its soffit height y_u and width b appears explicitly in the calculation and will affect the transient and steady-state results.

Fire geometry

The effects of changing the fire height from floor level to a point $h/4$ and $h/2$ is shown in Table 3 for a dimensionless heat input parameter of $Q^*=0.01$ and the standard door opening. The transient times not shown here are almost equal to that for the standard fire position. Changes in y_1 and (ρ_{h1}/ρ_1) result from the decreased entrainment of the fire plume.

Similar results are also shown in Table 4 where a comparison is presented of calculations for the standard point source plume and for a line plume with the same dimensionless heat addition rates. Again, time scales were almost equal for the two cases and the gross difference in y_1 and ρ_{h1}/ρ_1 results from the large difference in plume entrainment rates.

Hospital corridor case

As a final example, consider a two-room configuration in which the fire room (room 1) is connected to a much larger room (room 2). The connection between the rooms is the standard door ($y_u/h=0.813$ and $b/h=0.375$), and room 2 is connected to the outside only through a small leak (e.g. under a closed door) with an area about 6.5% of the area of this door. We arbitrarily assume that 40% of the heat input from the fire is lost to the walls in the fire room and that 20% of the enthalpy flux to the second room is transferred to the walls. The heat input from the fire grows linearly to a value of 111 kW at 375 s and remains constant thereafter. The dimensions of the first room are a height $h_1=2.5$ m and an area $S_1=20$ m^2, and the dimensions of the second room are $h_2=2.5$ m and $S_2=200$ m^2. Note that $S_2=10S_1$.

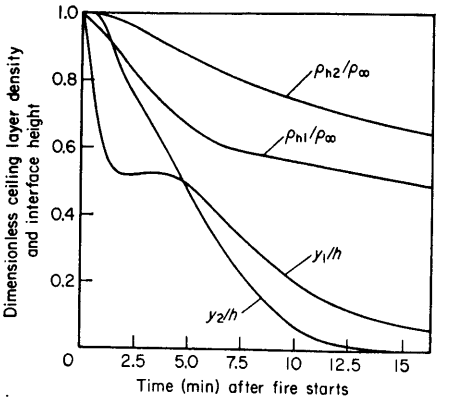

Figure 9. Hospital corridor example.

The ceiling layer density, normalized by the ambient density, and the interface height, normalized by the room height $h=2.5$ m, are shown as a function of the time in Fig. 9. The interface height in the fire room (y_1) drops rapidly in the first minute to a value of about $0.45h$ and remains at that level for about another 3 min. The interface height in room 2 falls to the same level at about 5 min and then both levels continue to fall rapidly. Remember that the heat input of the fire reaches its full value at 6.25 min. An interface height of $0.45h$ or about 1.13 m is probably slightly above the level of the head of a patient lying in a hospital bed.

For times greater than 5 min the interface height in room 2 is below that in room 1, and after 4.5 min the pressure distribution is such that hot ceiling layer gas from room 2 recirculates into room 1. The flow field is similar to that shown in Fig. 6(c) with the subscripts 1 and 2 reversed. To illustrate the flow field during this period, flow data are given in Table 5. Note that the flow of hot gas from room 2 back into room 1 is comparable to the corresponding cold flow.

The solutions are certainly not reasonable when $y_1<0.2h$ since the fire will extend into the ceiling layer and hence one would expect the plume model and perhaps the heat input rate to be incorrect. Also, values of ρ_{h1}/ρ_∞ less than 0.1–0.2 are not reasonable. Hence, the solution for $t>10$ m is not valid.

Table 3. Effect of fire elevation on ceiling layer height and density[a]

y_Q/h[b]	y_1/h	ρ_{h1}/ρ_∞
0	0.53	0.59
0.25	0.63	0.45
0.50	0.71	0.23

[a] $b=0.375h$, $y_u=0.813h$.
[b] y_Q is the height of fire origin above the floor.

Table 4. Comparison of ceiling layer height and density for line and point source fires[a]

Fire	Q^*	$Q_2{}^*$	y_1/h	ρ_{u1}/ρ_∞
Point source	0.01	—	0.59	0.53
Line source	—	0.01	0.24	0.72

[a] $b=0.375h$, $y_u=0.813h$.

Table 5. Flow conditions for hospital corridor example at 6.5 min

$y_1=1.01$ m and $y_2=0.79$ m	
Flow of hot gas from room 1 to room 2 (adjacent to soffit)	0.51 kg s^{-1}
Flow of hot gas from room 2 to room 1 (near interface)	0.20 kg s^{-1}
Flow of cool air from room 2 to room 1 (near floor)	0.27 kg s^{-1}

SUMMARY

We have presented a few results of numerical calculations carried out with a simple model which is being developed to predict the motion of combustion products and fresh air in a structure with a fire. We view this model as an element in a more ambitious calculation which will lead to the prediction of the spread of fire and combustion products through a complex building.

Acknowledgements

The model described in this paper has been developed under a grant from the Fire Research Center of the National Bureau of Standards and the authors were supported technically during their work by Dr John Rockett and Dr J. Quintiere of the Center.

REFERENCES

1. K. Kawagoe, Fire behavior in rooms. Report No. 27. Building Research Institute, Japan (1958).
2. P. H. Thomas, P. L. Hinkley, C. R. Theobald and D. L. Simms, Investigations into the flow of hot gases in roof venting. Fire Research Technical Paper No. 7. Department of Scientific and Industrial Research and Fire Offices' Committee Joint Fire Research Organization, Borehamwood (1963).
3. J. A. Rockett, *Combust. Sci. Technol.* **12**, 165 (1976).
4. J. G. Quintiere, B. J. McCaffrey and W. Rinkinen, *Fire Mater.* **2**, 18 (1978).
5. H. W. Emmons, H. E. Mitler and L. N. Trefethen, Computer fire code III. Home Fire Project Technical Report No. 25. Harvard University (1978).
6. E. E. Zukoski, Convective flows associated with room fires. California Institute of Technology, NSF Grant No. GI 31892X1. NSF RANN Conference on Fire Research, Harvard University (June 1975).
7. E. N. Tangren, W. S. Sargent and E. E. Zukoski, Hydraulic and numerical modeling of room fires. California Institute of Technology. NSF Grant No. ENV 76-06660 (June 1978).
8. E. E. Zukoski, *Fire Mater.* **2**, 54 (1978).
9. E. E. Zukoski and T. Kubota, A computer model for fluid dynamic aspects of a transient fire in a two-room structure. California Institute of Technology (January 1978).
10. B. R. Morton, G. I. Taylor and J. S. Turner, *Proc. R. Soc. London Ser. A* **234**, 1 (1956).
11. S. Yokoi, Study on the prevention of fire spread caused by hot upward current. Report No. 34, Building Research Institute, Japan (1960).
12. E. E. Zukoski and T. Kubota, Preliminary experiments concerning entrainment in a fire plume. California Institute of Technology (October 1979).
13. E. E. Zukoski and D. L. Peterka, Measurements of entrainment in a doorway flow. California Institute of Technology (October 1979).
14. J. Prahl and H. W. Emmons, *Combust. Flame* **25**, 369 (1975).

Received 25 May 1978; accepted in revised form 30 October 1979

APPENDIX: DEFINITIONS OF SYMBOLS

b	opening width
C_E	$(\pi C_v C_l^2)$; see Eqn (11)
C_T, C_v, C_l	constants in buoyant axisymmetric plume representation
C_J	constant in door-jet entrainment equation
C_{0i}	flow coefficient for flow through openings (see Eqn (13))
C_p, C_v	specific heats at constant pressure and constant volume
C_{T2}, C_{v2}, C_{l2}	constants in line plume representation
g	gravitational constant
h_i	height of ith room
L	length of line fire or plume
l_v	scale length for velocity distribution in plume
l_T	scale length for temperature distribution in plume
$\dot{m}_i$	sum of all mass fluxes into cool layer of room i
$\dot{m}_E$	entrainment rate of fire plume in cool layer
$\dot{m}_f$	fuel flow rate to fire
$\dot{m}_{hiJ}$	flow from hot layer of room i to hot layer of room J
$\dot{m}_{iJ}$	flow from cool layer of room i to cool layer of room J
$\dot{m}_J$	door-jet entrainment rate
$\dot{m}_{hi}$	sum of all mass fluxes *into* the hot layer of room i
P	pressure
$\dot{q}_i$	net heat and enthalpy flux to gas in the cool layer
$\dot{q}_{hi}$	net heat and enthalpy flux *from* gas in hot layer
Q	fire heat release rate
Q^*	dimensionless parameter, $Q/\rho_\infty C_p T_\infty \sqrt{g_{h1}}\, h_1^2$
Q_d^*	dimensionless parameter, $\dot{m}_{h1} C_p (T_{h1} - T_2)/\rho_2 C_p T_2 \sqrt{g Z_d}\, Z_d^2$
Q_z^*	dimensionless parameter, $Q/\rho_\infty C_p T_\infty \sqrt{gZ}\, Z^2$, for axisymmetric plume
Q_2^*	dimensionless parameter, $Q/\rho_\infty C_p T_\infty \sqrt{gZ}\, ZL$, for line plume
r	radial coordinate
R	gas constant for air
S_i	area of ith room
t	time
$\bar{t}$	dimensionless time, $\tau(h\sqrt{gh}/S)$
t^*	second dimensionless time, $\bar{t}Q^{*1/3}$
T_i	temperature of gas at location i
ΔT	difference between temperature of a plume and ambient temperature
$\overline{\Delta T}$	mass-averaged values of temperature difference in buoyant plume
w	vertical velocity in plume
y_Q	height of fire above floor
y_1 and y_2	height of interface in room 1 or 2
y_u and y_l	height to upper and lower edges of opening between rooms

$y_u\{I, i\}$	height to upper edge of opening i between room I and outside
$y_l\{I, i\}$	height to lower edge of opening i between room I and outside
Z	vertical coordinate
Z_d	vertical coordinate for door jet, $y_2 - y_0$
ρ	density

Subscripts

c	cold layer
h	hot layer
hi	property of hot layer in room i
i	property of cool layer in room $i = 1$ or 2
m	property on plume centerline for an axisymmetric plume
m2	property on plume centerline for a line plume
0	neutral buoyancy point in flames through an opening (see Fig. 3)
1 or 2	property in room 1 or 2
10	value when plume reaches ceiling in first room
∞	property of ambient gas